MAGNETOHYDRODYNAMICS Vol. 52 (2016), No. 3, pp. 379–389

ENGINEERING APPROACH TO NUMERICAL SIMULATION OF MHD HEAT TRANSFER

I.A. Belyaev, Y.I. Listratov, I.A. Melnikov, N.G. Razuvanov, V.G. Sviridov, E.V. Sviridov

Joined Institute of High Temperatures, Russian Academy of Sciences
13/2 Izhorskaya str., Moscow 125412, Russia

MHD heat transfer in liquid metal flow in heated channels with a cross-section of simple geometry (a round tube or a rectangular channel) affected by a magnetic field is investigated numerically using computational fluid dynamics (CFD) techniques. The approach is based on solving averaged Reynolds equations using the ANES20XE CFD code developed at the Moscow Power Engineering Institute.

List of symbols.

Coordinates:

x, y, z	Cartesian coordinates
r, φ, z	cylindrical coordinates

Vectors:

$\mathbf{u} = (u_x, u_y, u_z)$	velocity, [m/s]
$\mathbf{q}_{\mathrm{w}} = (q_{\mathrm{w}x}, q_{\mathrm{w}y}, q_{\mathrm{w}z})$	heat flux density on the wall, [W/m^2
$\mathbf{B} = (B_x, B_y, B_z)$	MF induction, [T]
$\mathbf{H} = (H_x, H_y, H_z)$	magnetic intensity, [A/m]
$\mathbf{D} = (D_x, D_y, D_z)$	electrical field induction, [C/m^2]
$\mathbf{E} = (E_x, E_y, E_z)$	electric intensity, [V/m]
$\mathbf{j} = (j_x, j_y, j_z)$	current density, [A/m^2]
$\mathbf{f}_{\mathrm{em}} = (f_{\mathrm{E}x}, f_{\mathrm{E}y}, f_{\mathrm{E}z})$	electromagnetic force, [N]
$\mathbf{f}_{\mathrm{A}} = (f_{\mathrm{A}x}, f_{\mathrm{A}y}, f_{\mathrm{A}z})$	buoyancy force, [N]

Scalars:

t	time, [s]
R_0	tube radius, [m]
D_0	tube diameter, [m]
U_{avr}	section averaged velocity, [m/s]
g	gravity, [m/s^2]
P	pressure, [Pa]
ξ	friction coefficient
T	temperature, [°C]
σ	intensity of temperature fluctuations, [°C]
σ_0	intensity of temperature fluctuations without MF, [°C]
T_{bulk}	bulk temperature, [°C]
α	heat transfer coefficient, [W/(m^{2}K)]
λ	thermal conductivity, [W/(mK)]
a	Temperature conductivity, [m^2/s]
μ_{m}	magnetic permeability, [H/m]
ε	permittivity
ν	kinematic viscosity, [m^2/s]
μ	dynamic viscosity, [kg/(ms)]

ρ	density, [kg/m^3]
σ_E	electrical conductivity, [(Ohm m)$^{-1}$]
C_p	heat capacity, [J/(kg K)]
β	thermal expansion coefficient, [1/K]
ρ_E	electric (charge) density, [C/m^3]
$\Theta_\mathrm{w} = \dfrac{\lambda(T - T_\mathrm{bulk})}{q_\mathrm{w} D_0}$	dimensionless wall temperature

Similarity criteria:

$\mathrm{Pr} = \dfrac{\nu}{a}$	Prandtl number
$\mathrm{Re} = \dfrac{U_\mathrm{avr} D_0}{\nu}$	Reynolds number
$\mathrm{Pe} = \dfrac{U_\mathrm{avr} D_0}{a} = \mathrm{Re} \cdot \mathrm{Pr}$	Peclet number
$\mathrm{Ha} = B_0 D_0 \sqrt{\dfrac{\sigma_\mathrm{E}}{\mu}}$	Hartman number
$\mathrm{Nu} = \dfrac{1}{\Theta_\mathrm{w}}$	Nusselt number
$\mathrm{Gr}_q = \dfrac{g\beta D_0^4 q_\mathrm{w}}{\lambda \nu^2}$	Grashof number

Indices:

tr	turbulent
lm	laminar
avr	averaged
w	wall

Introduction. A long-range program of magnetohydrodynamic (MHD) heat transfer investigation for nuclear power applications has been carried out at the Engineering Thermophysics Department (ETD) of the Moscow Power Engineering Institute MPEI [1]. At its early stage, the program had been focused on experiments because of poor performance of the computer hardware and experimental data unavailability for validation.

A unique test facility for investigating MHD heat transfer in the presence of a longitudinal or a transverse magnetic field has been designed and produced by the specialists of MPEI and Joint Institute of High Temperatures, Russian Academy of Sciences (JIHT RAS). A measurement technique has been developed and adjusted that enables us to obtain reliable date on hydrodynamics and heat transfer for a mercury flow affected by the magnetic field (MF). In 2014, the investigation of MHD heat transfer in round tubes was completed [1]. At present, experiments are being carried out in a plane channel [2] and in channels with a complicated cross-section [3]. A more powerful experimental facility is under development [1]. An extensive experimental database for the verification of numerical models and codes has been created based on vertical [1] and horizontal [4] tube configurations in a transverse MF and on tubes affected by a longitudinal MF [5].

The rapid evolution of computer facilities has made it possible to use an alternative approach to the investigation of the MHD heat transfer problem, namely, to solve the original problem using numerical modeling technique.

The solution of the Reynolds-averaged equations is among possible applications of numerical modeling. This technique provides a way of modeling the processes with a good enough accuracy using available computer capacities. However, such calculations need numerical relations or models to close the set of averaged equations, whereas these models and numerical codes should be very thoroughly verified.

1. Physical model.

1.1. Governing equations. We consider a flow of an electrically conducting viscous fluid (liquid metal). The flow is driven by an imposed pressure gradient so that the mean flow velocity U remains constant. The hydrodynamics and heat transfer for conducting liquid flow in the channel in the presence of a magnetic field is governed by the continuity (1), momentum (2), and energy (3) equations, by the Maxwell's equations (4)–(7) and Ohm's law (8) [6]:

$$\frac{\partial \rho u_k}{\partial x_k} = 0; \tag{1}$$

$$\left(\frac{\partial \rho u_i}{\partial t} + u_k \frac{\partial \rho u_i}{\partial x_k}\right) = -\frac{\partial P}{\partial x_i} + \frac{\partial}{\partial x_k}\left(\mu \frac{\partial u_i}{\partial x_k}\right) + \sum F_i; \tag{2}$$

$$\left(\frac{\partial \rho C_p T}{\partial t} + u_k \frac{\partial \rho C_p T}{\partial x_k}\right) = \frac{\partial}{\partial x_k}\left(\lambda \frac{\partial T}{\partial x_k}\right); \tag{3}$$

$$\varepsilon_{ikl} \frac{\partial H_l}{\partial x_k} = j_i; \tag{4}$$

$$\varepsilon_{ikl} \frac{\partial E_l}{\partial x_k} = -\frac{\partial B_i}{\partial t}; \tag{5}$$

$$\frac{\partial D_k}{\partial x_k} = \rho_E; \tag{6}$$

$$\frac{\partial B_k}{\partial x_k} = 0; \tag{7}$$

$$j_i = \sigma \left(E_i + \varepsilon_{ikl} u_k B_l\right). \tag{8}$$

The system of equations is written in a general form derived with the use of the low-frequency approximation. The bias current [6], the convection current in Ohm's law, the Coulomb component in the electromagnetic force are assumed negligible. Viscous and Joule dissipations are neglected in the energy equation (3). As to liquid metals, these assumptions are obvious and universally accepted.

Turbulent transport of momentum and energy can be conveniently described using the statistical approach, where the instantaneous velocity or the temperature are replaced by statistically averaged values [7]:

$$u_l = \bar{u}_l + \acute{u}_l; \quad P_l = \bar{P}_l + \acute{P}_l; \quad T_l = \bar{T}_l + \acute{T}_l.$$

The momentum equations derived by averaging Eqs. (1)–(3) with the use of this approach are the so-called Reynolds or averaged turbulent momentum equations (9), (10). These equations are supplemented with the energy equations (11) averaged in the same manner:

$$\frac{\partial \rho \bar{u}_l}{\partial x_l} = 0; \tag{9}$$

$$\left(\frac{\partial \rho \bar{u}_l}{\partial t} + \bar{u}_k \frac{\partial \rho \bar{u}_l}{\partial x_k}\right) = -\frac{\partial \bar{P}}{\partial x_l} + \frac{\partial}{\partial x_k}\left(\mu \frac{\partial \bar{u}_l}{\partial x_k}\right) + \sum \bar{F}_l - \frac{\partial}{\partial x_k}\left(\rho \overline{\acute{u}_l \acute{u}_k}\right); \tag{10}$$

$$\left(\frac{\partial \rho C_p \bar{T}}{\partial t} + \bar{u}_k \frac{\partial \rho C_p \bar{T}}{\partial x_k}\right) = \frac{\partial}{\partial x_k}\left(\lambda \frac{\partial \bar{T}}{\partial x_k}\right) - \frac{\partial}{\partial x_k}\left(\rho C_p \overline{\acute{u}_k \acute{T}}\right). \tag{11}$$

But these equations are not closed, in the sense that the correlations $\overline{u_l u_k}$ and $\overline{u_k T}$ are unknown. Therefore, the closure requires semi-empirical relations or model equations with empirical coefficients.

1.2. Closure relations. The liquid metal flow not subjected to the magnetic field is identical to a flow of any Newtonian fluid. There are many turbulence models of various sophistication levels. For the flow in channels of simple geometry, it is feasible to use simple algebraic relations, where the turbulent transport of momentum or energy is described with eddy viscosity. There are models based on the mixing length value for plane channels [8]. For ring-shaped tube, the Reichardt correlation can be recommended [7].

It is well known that the magnetic field suppresses turbulent transport. This effect can be described by the following coefficient [9]–[11]:

$$\left(\frac{\varepsilon_T}{\upsilon}\right)_{\mathrm{Ha}} = \gamma(\mathrm{Ha}, \mathrm{Re}) \left(\frac{\varepsilon_T}{\upsilon}\right)_{\mathrm{Ha}=0}.$$

It characterizes the turbulent fluctuation level in the presence of the magnetic field. The coefficient is derived in an assumption that the magnetic field suppresses turbulent transport evenly over the cross-section.

At present, two approaches are available to characterize this factor. The first one is based on the generalization of the friction factor data, whereas the second one involves turbulent fluctuations analysis.

The first approach is based on analysis of the friction factor behavior in the magnetic field. The MF effect on the friction factor is dual. On the one hand, the magnetic field suppresses turbulence (thereby, laminating the flow) hence decreasing the friction factor. On the other hand, an increase in friction factor due to the Hartman effect occurs in a transverse MF. Fig. 1 shows the friction factor for a conducting fluid flow in a round tube. The approach to the analytical correlation corresponds to full flow laminating.

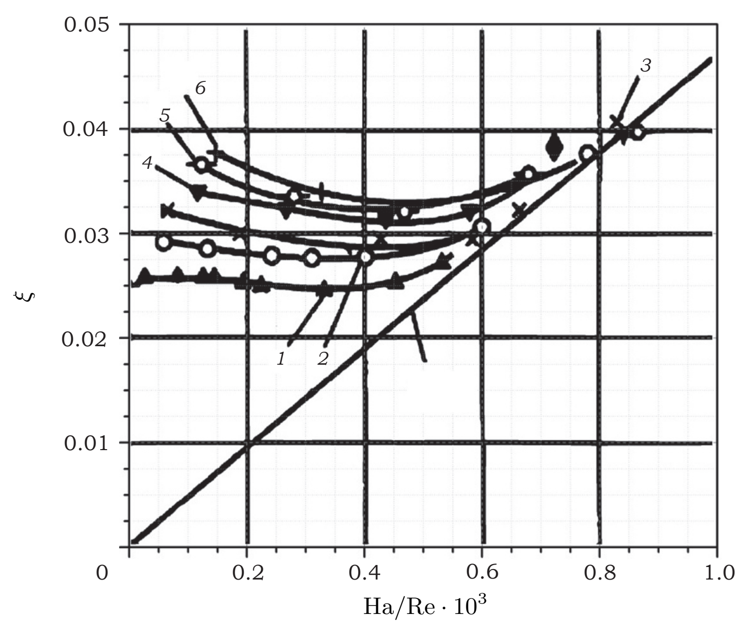

Fig. 1. The friction factor for round tube flow in a transverse magnetic field [12]. Re = 12000 (*1*), 7000 (*2*), 5000 (*3*), 3930 (*4*), 3325 (*5*), 2750 (*6*).

Table 1. Model coefficients.

MF orientation	Channel	Ha	k	n
Longitudinal	Plane channel [9]	$(40, 200]$	$7 \cdot \mathrm{Ha}^{-0.4}$	0.5
		$(200, 1000]$	$12 \cdot \mathrm{Ha}^{-0.42}$	0.6
	Round tube [10]	$(40, 200]$	$11 \cdot \mathrm{Ha}^{-0.4}$	0.5
		$(200, 10000]$	$14 \cdot \mathrm{Ha}^{-0.42}$	0.6
Transverse	Plane channel [11]	$(3, 20]$	$3.75 \cdot \mathrm{Ha}^{-0.7}$	0.8
		$(20, 100]$	0.46	0.8
	Round tube	–	–	–

The generalization of the experimental data for friction factor gives the required parameter $\gamma(\mathrm{Ha}, \mathrm{Re})$:

$$\gamma = \begin{cases} 1 - \exp\left[-k\left(\dfrac{\mathrm{Re} - \mathrm{Re}_{\mathrm{cr,Ha}}}{\mathrm{Re}_{\mathrm{cr,Ha}}}\right)^n\right], & \mathrm{Re} \geq \mathrm{Re}_{\mathrm{cr,Ha}} \\ 0 & \mathrm{Re} < \mathrm{Re}_{\mathrm{cr,Ha}} \end{cases} \tag{12}$$

where $\mathrm{Re}_{\mathrm{cr,Ha}}$ is the critical Reynolds number with the applied magnetic field; k, n are the coefficients (Table 1). The critical Reynolds number determines the transition from laminar to turbulent flow in the channels. Such models have been developed by the ETD specialists for simple geometry channels exposed to longitudinal and transverse magnetic fields. The critical Reynolds number in case of the longitudinal magnetic field for round tubes could be defined as

$$\mathrm{Re}_{\mathrm{cr,Ha}} = \mathrm{Re}_{\mathrm{cr,Ha=0}}\left[0.5 + \sqrt{\frac{1}{4} + \frac{0.4\mathrm{Ha}^2}{\mathrm{Re}_{\mathrm{cr,Ha=0}}}}\right], \tag{13}$$

where $\mathrm{Re}_{\mathrm{cr,Ha=0}}$ is the critical Reynolds number without the magnetic field. For the plane channel flow exposed to the transverse magnetic field the following expression can be recommended [6]

$$\mathrm{Re}_{\mathrm{cr,Ha}} = 1125\left[1 + \sqrt{1 + 0.92\mathrm{Ha}^2}\right]. \tag{14}$$

The second approach is based on analysis of local turbulent fluctuations in the flow. Let us consider temperature waveforms (Fig. 2) and the distribution of the temperature fluctuation intensity (Fig. 3) for liquid metal flow in the heated channel. It is assumed that natural convection has no considerable effect on the flow. Hence, the reason of temperature fluctuations is the flow turbulence. The application of the magnetic field decreases the temperature fluctuation intensity that is evident from the figures.

The generalization of the data on temperature fluctuation intensity also makes it possible to determine the extent of turbulence suppression in the magnetic field:

$$\gamma_{\mathrm{T}}(\mathrm{Ha}, \mathrm{Re}) = \exp\left\{\frac{1}{2}\frac{\mathrm{Ha}^2}{\mathrm{Re}}\right\}.$$

The derived expressions for $\gamma(\mathrm{Ha}, \mathrm{Re})$ and $\gamma_{\mathrm{T}}(\mathrm{Ha}, \mathrm{Re})$ were utilized when modelling the MHD flow in the channels of simple geometry. Nowadays many software packages have been developed for solving the system of equations – using

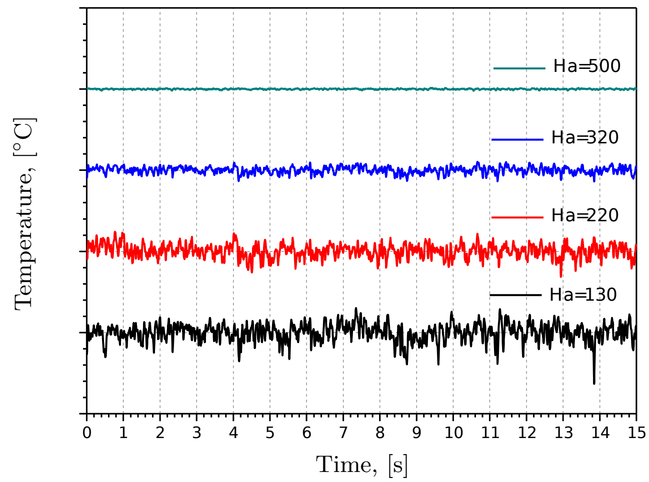

Fig. 2. Temperature fluctuations in a transverse magnetic field [14].

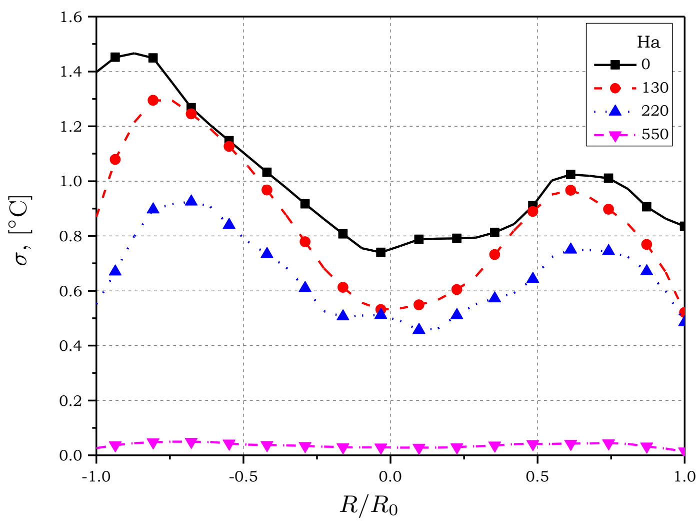

Fig. 3. Temperature fluctuation intensity distribution over the cross-section [14].

various methods. A wide variety of available software for numerical modelling impresses even the most sophisticated designer. The authors of the current paper have selected the noncommercial application software code ANES20XE developed at and supported by the ETD at MPEI [15]. This code is a control volume (CV) solver.

2. Solved equations. The system of averaged equations for liquid metal flow in the presence of the magnetic field can be reduced to six governing equations which can be conveniently written in the following form: the continuity equation (14), the three momentum equations for the i-th component of velocity (15), the energy equation (16), and the electrical potential equation (17):

$$\frac{\partial \rho u_i}{\partial t} + \mathrm{div}(\rho \mathbf{u}) = 0; \tag{15}$$

$$\frac{\partial \rho u_i}{\partial t} + \mathrm{div}\left(\rho \mathbf{u} u_i\right) = -\frac{\partial P}{\partial x_i} + \mathrm{div}\left[\left(\mu + \mu_{\mathrm{T}}\right) \nabla u_i\right] + \sum f_i; \tag{16}$$

$$\frac{\partial \rho C_p T}{\partial t} + \operatorname{div}\left(\rho \mathbf{u} C_p T\right) = \operatorname{div}\left[\left(\lambda + \lambda_{\mathrm{T}}\right) \nabla T\right]; \tag{17}$$

$$0 = \operatorname{div}\left(\nabla \Phi\right) - \operatorname{div}\left(\mathbf{u} \times \mathbf{B}\right), \tag{18}$$

where λ_{T}, μ_{T} are the eddy viscosity and the eddy conductivity, respectively; f_i is the mass force. When a liquid metal runs in the presence of a magnetic field, an additional electromagnetic force, acting on the flow, is induced. It can be calculated by the following expression

$$\mathbf{f}_{\mathrm{e}} = \mathbf{j} \times \mathbf{B}.$$

The fact that the flow is not isothermal can be accounted for by specifying the variable properties in Eqs. (13)–(16) or using certain approximations. The Boussinesq approximation [7] in which the density non-uniformity is considered only in the buoyancy force is the most widely accepted one:

$$\mathbf{f}_{\mathrm{g}} = -\beta \rho \left(T - T_{\mathrm{ARH}}\right) \mathbf{g}, \quad \mathbf{g} = g \mathbf{e}_{\mathrm{g}}.$$

where $\mathbf{e}_{\mathrm{g}}$ is the unit vector in the direction of gravity.

3. Numerical simulation of liquid metal flow in a transverse magnetic field. For example, we consider a mercury downward flow in a vertical round heated tube in a transverse magnetic field. The MHD configuration of the flow is illustrated in Fig. 4. The numerical domain includes the channel and its wall.

The Reichardt velocity distribution is set at the tube inlet [7]. The no-slip condition for the velocity is set on the tube wall. The fluid temperature at the tube inlet is assumed to be constant. There is the heated and magnetic field affected section after the entrance section. Along the Y-axis a uniform value of the magnetic field induction is set. The heat flux is prescribed outside the heated tube section:

$$q = \begin{cases} q_{\mathrm{w}1}, & 0 \le \varphi < \pi/2, 3\pi/2 \le \varphi < 0; \\ q_{\mathrm{w}2}, & \pi/2 \le \varphi < 3\pi/2. \end{cases}$$

The boundary conditions for the electric potential on the tube outside wall is $\partial\Phi/\partial n$. The reference point for the potential is $\Phi = 0$ at the tube inlet. The

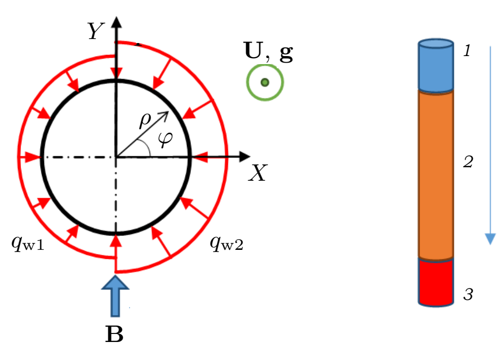

Fig. 4. Flow configuration. *1* – entrance section, *2* – heated and magnetic field affected section, *3* – exit section.

domain includes also a tube wall, where the energy and potential equations are solved.

The mass flow at the channel inlet is fixed. The pressure boundary at the outlet is $P = 0$. The equations are solved by the SIMPLE method.

To simplify the problem, we did not consider the inlet effect and the magnetic field induction non-uniformity. The heat flux distribution along the perimeter of the tube was also simplified (see Fig. 4).

4. Results and discussion. Some test calculations were performed to find the optimal mesh geometry and density. From the practical point of view, main attention was focused on the local wall temperature distribution. We considered the fixed cross-section ($z/D_0 = 37$) which matches with the outlet of the heated part of the tube, where the magnetic field was constant. The heat transfer was already stable in this section, and a lot of experimental data was sampled there.

For the beginning, we considered the test calculations of hydrodynamics and heat transfer without the magnetic field. The availability of reliable experimental data on hydrodynamics and heat transfer (the Layon dependence, for example, Eq. (19)) allowed to verify our code.

Fig. 5 shows the distribution of the dimensionless wall temperature (calculated and measured). The data were obtained for the mode with $\mathrm{Re} = 3.5 \cdot 10^4$, $\mathrm{Ha} = 0$, $\mathrm{Gr} = 0.6 \cdot 10^8$.

We observed a good agreement of our results with the experimental data. The obtained averaged heat transfer coefficients for some modes are displayed in Fig. 6. As seen, they match with the Layon formula as well:

$$\mathrm{Nu} = 7 + 0.025\mathrm{Pe}^{0.8}. \tag{19}$$

Then we investigated the dependence of mesh density on the calculated results. The wall temperature of two grid types (Cartesian and cylindrical) is compared with the experimental data in Fig. 7. During the numerical experiments, the optimal mesh density was determined to be approximately 1 million control volumes. This provided the required accuracy with a reasonable time of the calculation.

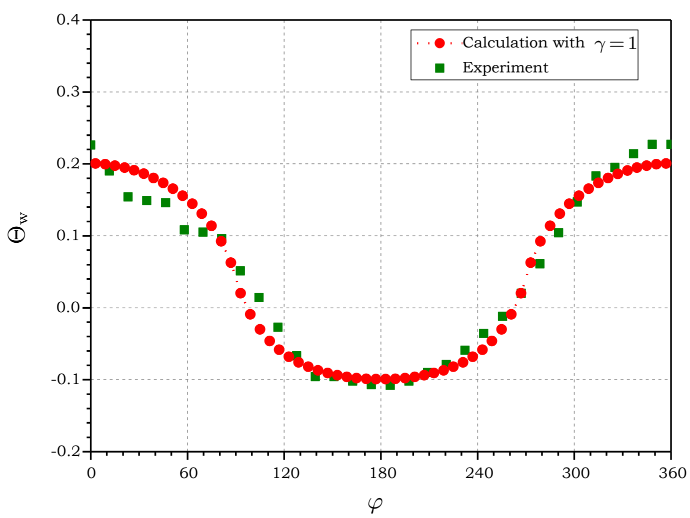

Fig. 5. Dimensionless wall temperature distribution ($\mathrm{Re} = 3.5 \cdot 10^4$, $\mathrm{Ha} = 0$, $\mathrm{Gr} = 0.6 \cdot 10^8$).

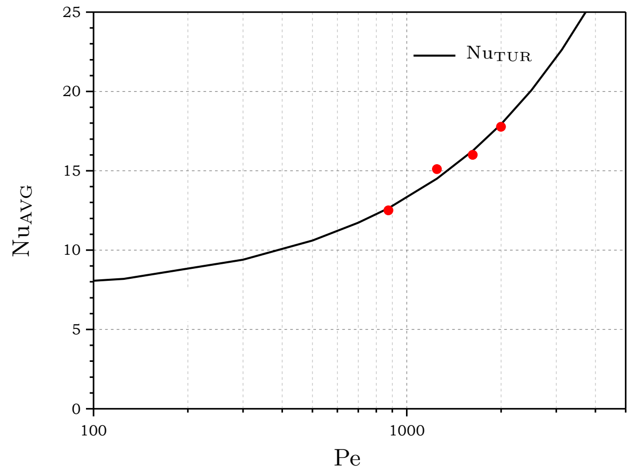

Fig. 6. The heat transfer coefficient vs. the Peclet number ($\mathrm{Gr} = 0.6 \cdot 10^8$).

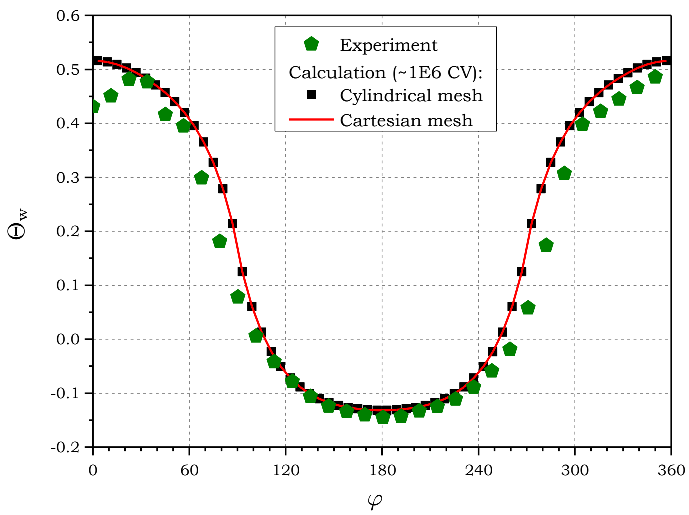

Fig. 7. Dimensionless wall temperature distribution. The transverse magnetic field ($\mathrm{Re} = 3.5 \cdot 10^4$, $\mathrm{Ha} = 320$, $\mathrm{Gr} = 0.6 \cdot 10^8$).

After that we calculated the flow in a strong transverse magnetic field. The wall temperature distribution for this case is compared in Fig. 8.

In the numerical experiments, a good qualitative and quantitative agreement between the results of calculations, the experimental data and the analytical estimations was obtained.

5. Conclusion. An engineering approach to MHD heat transfer simulation has been developed. The approach describes numerical modelling of MHD heat transfer in simple geometry channels. The effect of the magnetic field on turbulent fluctuations is taken into account using the intermittency factor derived from the experimental data. The results of the numerical investigations are in good agreement with the available experimental data and enable their gaps to be filled in. The proposed approach allows to generalize the results of the experimental programs and to predict feasible result outside the range of the verified regime parameters.

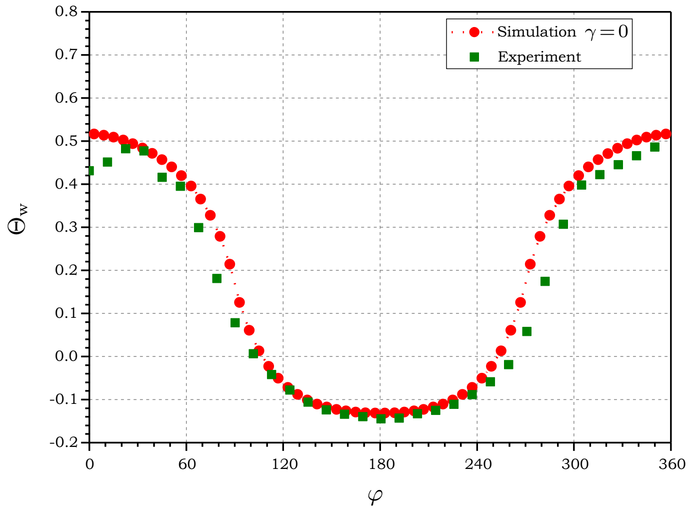

Fig. 8. Wall temperature distribution. The transverse magnetic field ($\mathrm{Re} = 3.5 \cdot 10^4$, $\mathrm{Ha} = 320$, $\mathrm{Gr} = 0.6 \cdot 10^8$).

The approach could be improved by extending the range of simulated MHD phenomena (including temperature fluctuations and reverse flow genesis). It is a topic for the further research.

Acknowledgements. The study is supported by RSCF project No. 14-50-00124.

References

[1] V.M. Batenin, I.A. Belyaev, V.G. Sviridov, E.V. Sviridov, Y.I. Listratov. Modernization of the experimental base for studies of MHD heat exchange at advanced nuclear power facilities. *High Temperature*, vol. 53 (2015), no. 6, pp. 904–907.

[2] I.R. Kirillov, D.M. Obukhov, L.G. Genin *et al.* Buoyancy effects in vertical rectangular duct with coplanar magnetic field and single sided heat load. *Fusion Engineering and Design*, vol. 104 (2016), pp. 1–8.

[3] I.A. Belyaev, L.G. Genin, S.G. Krylov *et al.* Experimental investigations of heat transfer and temperature fields in models simulating fuel assemblies used in the core of a nuclear reactor with a liquid heavy-metal coolant. *Thermal Engineering*, vol. 62 (2015), no. 9, pp. 645–651.

[4] I.A. Belyaev, Yu.P. Ivochkin, Ya.I. Listratov, N.G. Razuvanov, and V.G. Sviridov. Temperature fluctuations in a liquid metal magnetohydrodynamic flow in a horizontal inhomogeneously heated tube. *High Temperature*, vol. 53 (2015), no. 5, pp. 735–742.

[5] I.A. Belyaev, L.G. Genin, Y.I. Listratov *et al.* Specific features of liquid metal heat transfer in a Tokamak reactor. *Magnetohydrodynamics*, vol. 49 (2013), nos. 1–2, pp. 177–190.

[6] L.G. Genin, V.G. Sviridov. *Hydrodynamics and Heat Transfer of MHD Flows in Channels* (MPEI Publishing House, Moscow, 2001), 200 p. (in Russian).

[7] E.P. Valueva, V.G. Sviridov. *Introduction to Fluid Mechanics: Textbook for Universities* (MPEI, Moscow, 2001), 300 p. (in Russian).

[8] S.V. Patankar, S. Acharya. Development of a turbulence model for rectangular passages. *Trans. CSME*, vol. 8 (1984), p. 46.

[9] L.G. Genin, T.E. Krasnoshekova. Fluid flow and heat transfer in the flow of electrically conducting fluid in a plane channel in a longitudinal magnetic field. *MPEI Vestnik*, (1998), no. 3, pp. 59–62 (in Russian).

[10] L.G. Genin, I.E. Krasnoshekova, L.V. Petrina. The hydrodynamics and heat exchange of an conducting fluid in a tube within a longitudinal magnetic field. *Magnetohydrodynamics*, vol. 26 (1990), no. 1, pp. 50–56.

[11] E.V. Sviridov. *Investigation of Hydrodynamic and Heat Transfer During Liquid Metal Flow in the Presence of Transverse Magnetic Field* (PhD Thesis, 2002, Moscow, MPEI), 102 p. (in Russian).

[12] Yu.M. Gelfgat, O.A. Lielausis, E.V. Shcherbinin. *Liquid Metal under the Action of Electromagnetic Forces* (Zinatne Publishing House, Riga, 1976), 246 p. (in Russian).

[13] F.W. Fraim, W.H. Heiser. The effect of a strong longitudinal magnetic field on the flow of mercury in a circular tube. *J. Fluid Mech.*, vol. 33 (1968), no. 2, pp. 397–413.

[14] I.A. Melnikov. *Hydrodynamic and Heat Transfer Investigation of MHD Flows in a Vertical Tube in the Presence of Transverse Magnetic Field* (PhD thesis, Heat 2014, Moscow, MPEI), 102 p. (in Russian).

[15] V.I. Artemov, A.G. Murov, V.I. Shikov, G.G. Yankov. *The automation system of numerical experiment ANES: ideology and architecture* (Preprint no. 8-247, Moscow IHT AS USSR, 1988) (in Russian).

Received 11.04.2016